Two-stage Rydberg charge exchange in a strong magnetic field

M. L. Wall, C. S. Norton, and F. Robicheaux
Department of Physics, Auburn University, Auburn, Alabama 36849-5311, USA
(Received 21 June 2005; published 4 November 2005)

We have performed calculations of two successive charge transfers from Rydberg states in a strong magnetic field. In the first charge transfer, a positron interacts with a highly excited atom to form positronium. In the second stage, the positronium interacts with an antiproton to give antihydrogen. For many parameters, our results are in qualitative agreement with previous calculations with no magnetic field. However, we do find that there are important changes which may affect the usefulness of the method for efficient formation of antihydrogen that can be trapped.

DOI: 10.1103/PhysRevA.72.052702 PACS number(s): 34.60.+z, 32.80.Cy, 32.60.+i

I. INTRODUCTION

Recent experiments have demonstrated the formation of antihydrogen ($\bar{H}$) (e.g., see Refs. [1,2]). In both experiments, cold antiprotons, $\bar{p}$'s, traverse a cold positron, e^+, plasma; a $\bar{p}$ can capture one of the e^+'s during its brief time in the plasma. Presumably [3–5], the $\bar{H}$ is formed through three body capture since this mechanism has the largest rate for the parameters of the experiments. In three body capture, e^+'s scatter in the field of a $\bar{p}$ so that an e^+ loses enough energy to become bound to the $\bar{p}$. In both experimental apparati, the $\bar{p}$ start with a relatively large kinetic energy and slow down through their interaction with the e^+ plasma. A simulation [6] of the slowing mechanisms and the three body capture found that the $\bar{H}$ typically formed with energies much larger than the thermal energy of the e^+'s because the $\bar{p}$'s did not thermalize before the capture. This result was seen in both experiments [7,8]. The relatively high kinetic energy of the $\bar{H}$ will make it difficult to trap. Neutral particles are typically trapped using their magnetic moment. Taking the Bohr magneton times a 1 T magnetic field change as the unit of energy gives a well depth of $\sim 3/4$ K.

A different method for the formation of $\bar{H}$ was suggested in Ref. [9]. This method used a two-stage charge transfer to attach the e^+ to the $\bar{p}$. Reference [9] suggested that a beam of Rydberg atoms be directed through an e^+ plasma that is close to trapped $\bar{p}$'s. When the Rydberg atom enters the e^+ plasma, a charge exchange quickly occurs giving a highly excited positronium (Ps). A fraction of the Ps population travels to the region of the trapped $\bar{p}$'s where a second charge exchange can occur. The trapped $\bar{p}$'s can be cooled to temperatures near 4 K. Because the kinetic energy of the $\bar{H}$ is mostly determined by the kinetic energy of the $\bar{p}$ just before the charge exchange, the $\bar{H}$ formed in the two-stage charge exchange are likely moving less rapidly than when formed by three body capture. In a recent paper [10], the ATRAP Collaboration reported a successful implementation of this two-stage charge transfer method for $\bar{H}$ formation.

In the original theoretical treatment of this process [9], the charge transfers occur in zero magnetic field. As noted in the experiment [10], the magnetic field in actual measurements of $\bar{H}$ production is large enough to strongly change the internal atomic states. Although the magnetic fields are only $B \sim 1$–5 T, the atomic states are highly excited; in Ref. [10], the principal quantum number $n \sim 40$. Thus it is not clear which (if any) of the computed properties of this process [9] are changed due to the strong magnetic field. It is the purpose of this paper to reexamine the two-stage charge exchange but now include the strong magnetic field in the calculations. In addition, we want to discover if the magnetic field introduces any interesting features into this process.

As in Ref. [9], we will use a classical trajectory Monte Carlo (CTMC) method to compute the properties of the Ps and $\bar{H}$. This should be an accurate method because the states that are involved have large quantum numbers: for example, $n \sim 40$. To simplify the discussions, we will assume the magnetic field is in the z direction.

II. COMPUTATIONAL METHOD

In this section, we describe the various parts of the calculation that determine the accuracy and applicability of our results.

A. Numerical method

In our numerical simulation, we utilized the adaptive step size, fourth-order Runge-Kutta time propagation scheme [11]. We checked the accuracy of each trajectory by comparing conserved quantities (e.g., total energy) at the end of the trajectory to that at the beginning. Any trajectory with a change in a conserved quantity larger than 0.1% was rejected from our sample. Our rejection rate was very low and should not affect our results; for example, only 2–3 % of the trajectories that gave a charge exchange were rejected for $n=40$ at $B=4$ T. We used the full equations of motion for the light particles since it was not clear how accurate various approximations (e.g., the guiding center approximation) would be for all of the fields and energies in our calculations.

We approximated the interaction of the Cs^+ ion with the electron (e^-) and e^+ as being a pure Coulomb force for all distances. This is clearly a poor approximation when either the e^- or e^+ is within $\sim 10^{-10}$ m of the nucleus. However, the number of trajectories that traverse this region is small for the highly excited states used in practice and all of the inter-

esting physics occurs when both light particles are far from the nucleus. Thus we expect this approximation to be very good for the results reported below.

B. Initial distribution

We first simulated the production of Ps through charge exchange from highly excited cesium (Cs) to an approaching e^+. In this stage, we considered the Cs nucleus as an infinitely massive, fixed body. This should be a good approximation because the e^+ speed is more than 10 times that of the atom; also, the motional Stark field, vB, for the atom is only several V/cm which is less than that needed to n-mix states near $n\sim 40$. The Cs is in a highly excited state, but the position and velocity distribution of the highly excited e^- is not known. The atom is laser excited to a specific $n\ell$ state, but travels through fields (which can mix the ℓ states) and then interacts with many e^+'s (which strongly mixes ℓ and more weakly mixes n) before a charge transfer takes place to give Ps. We have assumed the e^- on the atom is at the energy of a specific n-state but that the angular momentum has been randomized.

The e^+ was fired at the highly excited Cs atom. The z position ($\vec{B}\equiv B\hat{z}$) of the e^+ is started 20 times the size of the atom from the nucleus with a random shift; the shift is to randomize the time that the e^+ reaches the atom and is between 0 and the speed of the e^+ times the Rydberg period of the atom. The (x,y) position of the e^+ was random within a square with an edge length 14 times the size of the atom plus the cyclotron radius of the e^+. The e^+ velocities were initialized using the Maxwell-Boltzmann distribution at a temperature of 4 K for all three velocity components. The propagation was terminated when the magnitude of the difference of the z positions of the e^+ and Cs^+ differed by more than 20 times the size of the atom. When the e^+ reached this point, it was clear whether or not it had captured the e^- by checking the distance between the e^+-e^-. From these initial conditions, we calculated approximately 100 000 recombined e^--e^+ pairs and subsequent trajectories.

In our second charge exchange, we simulated the formation of $\bar{H}$ by having the highly excited Ps calculated from the first stage interact with a stationary, infinitely massive $\bar{p}$. Treating the $\bar{p}$ as being infinitely massive and stationary should be a good approximation since the $\bar{p}$'s speed is more than a factor of 20 less than that of the light particles. To simulate the collision of the Ps with the $\bar{p}$, we need to ensure that the impact parameter and time of the collision is randomized. To achieve this, we first shifted the center of mass position to the origin and propagated the Ps backwards in time until the z component of the center of mass position was equal to twenty times the size of the atom. Then we introduced an antiproton at the origin, and shifted the x, y, and z positions of the Ps by a random amount. This random amount was on the order of 10 times the original size of the excited Cs atom, and was oriented in the direction perpendicular to the Ps motion; this effectively randomizes the impact parameter of the Ps-$\bar{p}$ collision. We then propagated the Ps forward in time until the e^- reached a distance from the $\bar{p}$ of 35 times the size of the atom in the z direction. At this point, it was clear whether or not the $\bar{p}$ had captured the e^+ to form $\bar{H}$.

III. RESULTS

We computed statistics associated with the physical properties of the Ps and $\bar{H}$ formed in our simulation, such as angular momenta and internal energy. We present results on the properties of the Ps and $\bar{H}$ that will affect the usefulness for $\bar{H}$ experiments or whose general trend contain unexpected features. In particular, we calculated the rates at which Ps and $\bar{H}$ were produced in the simulation, when the system was subject to various changes in initial conditions, such as temperature and magnetic field strength. We also computed the binding energy and L_z distribution of the $\bar{H}$; these quantities are important for the possibility of trapping the $\bar{H}$.

A. Ps properties

Simple estimates show that the Ps formation rate will be sufficiently high that in many cases it is not a consideration since all atoms entering the e^+ plasma will experience a charge exchange. However, it is still worthwhile to have simple expressions for these rates. Another important consideration is the distribution of directions in which the Ps emerge; the strong B field provides a direction in space and we find that the Ps do not necessarily emerge isotropically.

1. Total Ps formation rate

We used our simulated trajectories to compute the charge transfer rate, $\langle v\sigma\rangle$ when an e^+ collides with a highly excited atom. The natural scale of the rate is the squared size of the atom times the thermal velocity of the e^+. This leads us to examine the rates as a dimensionless constant times these parameters:

$$\langle v\sigma\rangle(n,T,B)\equiv C(n,T,B)(2n^2a_0)^2\sqrt{k_BT/m}, \qquad (1)$$

where C is the dimensionless constant, n is the principal quantum number, T is the temperature of the e^+, B is the magnetic field, k_B is Boltzmann's constant, and m is the mass of the e^+.

We performed calculations for $n=30,40,50$, $B=1,2,4$ T, and temperatures of 4 and 8 K. We found the rate coefficient to be in the range $4<C<6.5$. This is comparable to the "velocity averaged" cross section of $9.7\pi n^4a_0^2$ found in Ref. [9] for zero magnetic field.

2. Angle of Ps emergence

We computed the directions that the Ps traveled after the charge transfer. When the Ps reached a distance from the nucleus of 25 times the size of the original atom, we computed the direction of motion from $\theta=\arctan(\rho/|z|)$ where z is the distance along the magnetic field and ρ is the distance perpendicular to the field. We obtained similar angular distributions when we computed the direction at larger distances.

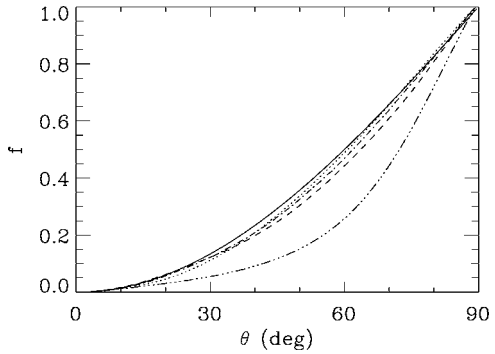

FIG. 1. The fraction of Ps that travel in a direction with angle less than θ relative to the magnetic field. The dotted line is for $B=1$ T and the Rydberg atom initially in $n=30$, the dashed line is for $B=4$ T, $n=30$, the dash-dot line is for $B=1$ T, $n=40$, and the dash-dot-dot-dot line is for $B=4$ T, $n=40$. The solid line is $1-\cos\theta$ which is the isotropic distribution. Note that the $B=4$ T, $n=40$ case gives relatively few atoms traveling along the magnetic field.

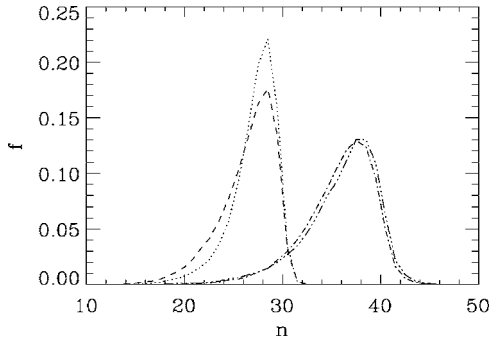

FIG. 2. The fraction of $\bar{H}$ formed with energies corresponding to principal quantum number n. The lines are for the same cases as in Fig. 1. The magnetic field does not strongly affect the binding energy of the atoms. The peak is slightly shifted down in n from that of the initial atom.

In Fig. 1, we show the fraction of trajectories that emerge with angle less than θ for a few values of n and B for $T=4$ K. An isotropic distribution gives $1-\cos\theta$ which is shown for comparison. For the $B=1$ T cases and for $n=30$ and $B=4$ T, the angular distribution is roughly isotropic. However, the $n=40$, $B=4$ T case (which is most similar to the experiment in Ref. [10]) clearly departs from isotropic. There is a strong suppression of Ps emergence at small angles. This means fewer Ps are available to travel along the magnetic field for the second stage of this process. For the case when the system is most strongly perturbed by the magnetic field, the Ps are much more likely to emerge perpendicular to the field than would be expected from an isotropic distribution. The next stage of $\bar{H}$ experiments will attempt to trap the $\bar{H}$ which means the magnetic fields will be lowered to ~ 1 T; our data suggest that the suppression of travel along the magnetic field will not be strong as long as $n \leqslant 40$ are used.

The suppression of small angle Ps for $n=40$ and 4 T field is the opposite of naive expectations which suggest that a larger fraction of Ps should emerge at small angle because the light particles should be pinned to the B-field lines. The simulations include the full motion of the light particles so the origin of the suppression of motion along the magnetic field is somewhat uncertain. We note that the velocity of the Ps without the B field would be roughly the thermal velocity of the e^+ which is roughly 7 km/s. Compare this with the drift velocity of the guiding center approximation of Ps; at this level, the electric field at the e^- due to the e^+ gives an $\vec{E}\times\vec{B}$ drift and the electric field at the e^+ due to the e^- gives exactly the same drift. If the binding energy of the Ps is approximately that of the Rydberg atom, this gives a drift speed of $e/(4\pi\epsilon_0 r^2 B) \sim 50$ km/s for $n=40$. The Ps that could be best approximated by the guiding center approximation would have the largest e^+-e^- separation perpendicular to the B field. We find that the Ps with the largest θ are those that are best described by the guiding center approximation. Simple estimates suggest the $\vec{E}\times\vec{B}$ drift velocity decreases like $1/n^4$. Therefore, we expect that the small angle suppression will be reversed to become an enhancement for higher n than in our simulation.

B. $\bar{H}$ properties

In the second stage of this process, a Ps collides with a $\bar{p}$ to give a $\bar{H}$ and an e^-. We have computed the properties of the resulting $\bar{H}$ using the full population of Ps.

1. Distribution of n

In Fig. 2, we show the distribution of principal quantum numbers of the $\bar{H}$ for the same n, B, and T as in Fig. 1. As in the zero field calculation [9], the population is peaked slightly below the original n of the Rydberg atom. The distribution over n is somewhat broad as in the zero field calculation. We note that the lower n states radiate much faster than the higher n states. Thus, the tails of the distribution on the low-n side may be important for the goal of reaching ground state $\bar{H}$.

2. Distribution of L_z

The goal of the next generation of $\bar{H}$ experiments is to trap the antimatter and build up a substantial number for precision spectroscopy experiments. To this end, multipole magnetic fields will be added to the present nested Penning traps. The geometry will be such that the B field will have its smallest magnitude near the center of the trap; the B field will increase in magnitude toward the walls of the trap. Also, mirror coils will be added so the magnitude of the B field increases when moving along the trap axis away from the e^+ plasma. This should allow the trapping of sufficiently cold atoms that are in the low field seeking geometry. For the highly excited states of $\bar{H}$, low field seeking states have negative L_z.

In Fig. 3, we show the distribution of $L_z=m(xv_y-yv_x)$ for the same n, B, and T as in Fig. 1. Note that the peak of the distribution is at positive L_z for all cases. The majority of $\bar{H}$ are in high field seeking states and thus these atoms will be *attracted* to the walls of the trap. For $n=30$ and $B=1$ T,

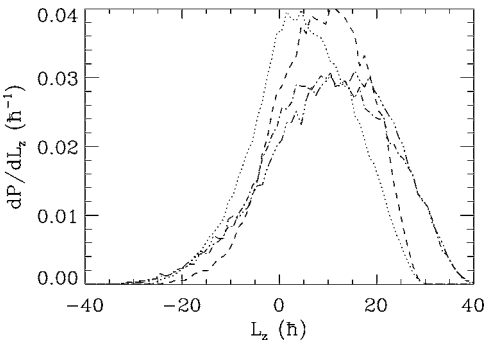

FIG. 3. The distribution of $\bar{H}$ formed with the positron having angular momentum, $L_z=m(xv_y-yv_x)$, along the B field. The lines are for the same cases as in Fig. 1. Unlike the $B=0$ case, the L_z is not centered at 0. The implications are discussed in the text.

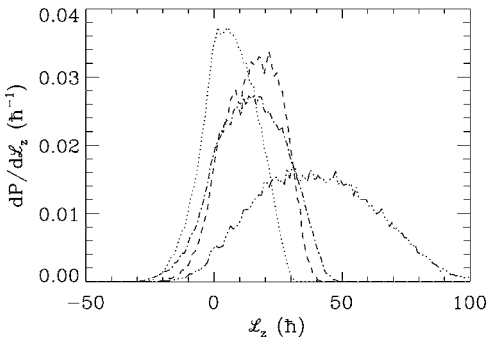

FIG. 4. The distribution of $\bar{H}$ formed with the positron having canonical angular momentum, $\mathcal{L}_z=L_z+qB(x^2+y^2)/2$, along the B field. The lines are for the same cases as in Fig. 1. The canonical angular momentum $\mathcal{L}_z$ is conserved whereas L_z is not. Also, the $\mathcal{L}_z$ is the angular momentum in the Hamiltonian and in the quantized atom. The implications are discussed in the text.

approximately 31% of the $\bar{H}$ have negative L_z while the fraction drops to approximately 20% for the other cases.

Actually, the situation is somewhat worse than depicted in Fig. 3. This is because the z-component of the angular momentum is not conserved. It is the z component of the canonical angular momentum $\mathcal{L}_z=L_z+qB(x^2+y^2)/2$ which is the conserved quantity [12]. The canonical momenta (and the angular momenta constructed from them) are the quantities that appear in the Hamiltonian and have the quantum analog. Because $q=+e$ for e^+, $\mathcal{L}_z>L_z$. In Fig. 4 we show the distribution of $\mathcal{L}_z$ for the same n, B, and T as in Fig. 1. The distribution for $n=30$, $B=1$ T hardly shifts, but the others shift by noticeable amounts. For $n=30$ and $B=1$ T, approximately 27% of the $\bar{H}$ have negative $\mathcal{L}_z$ while the fraction drops to approximately 15% for $n=40$, $B=1$ T, 9% for $n=30$, $B=4$ T, and 3% for $n=40$, $B=4$ T.

Although L_z is a better guide for whether the $\bar{H}$ is attracted to high B fields or low B fields, we think the distribution of $\mathcal{L}_z$ is important for trapping. This is because as the $\bar{H}$ radiates the $\mathcal{L}_z$ changes by $\pm\hbar$ or $0\hbar$. If the $\bar{H}$ starts with positive $\mathcal{L}_z$, it will tend to continue to be positive. This propensity coupled with the fact that $\mathcal{L}_z\rightarrow L_z$ as n decreases means that the $\bar{H}$ will go through a stage of being attracted to high B fields during the radiative cascade. Thus, simple (statistical) estimates of the fraction of $\bar{H}$ available for trapping will likely be too large.

IV. CONCLUSIONS

We have simulated the formation of $\bar{H}$ through a two stage charge exchange mechanism. In the first stage, e^+ collide with highly excited atoms resulting in a charge exchange that gives highly excited Ps. We found that the rate of formation is roughly what would be expected from geometric arguments. However, we found that the Ps do not necessarily emerge isotropically but can have a preference for moving perpendicular to the magnetic field for some n and B. This appears to be due to a uniform velocity that arises from the $\vec{E}\times\vec{B}$ drift where the $\vec{E}$ at the e^- is from the e^+ and vice versa.

We found that the $\bar{H}$ that forms when the Ps collides with a $\bar{p}$ has a distribution of principal quantum numbers peaked near the initial n of the excited atom in the first stage. This is similar to the results found in the field free case [9]. However, we found the distribution of L_z definitely peaked at positive values. Positive L_z gives $\bar{H}$ that are attracted to high magnetic field. This means that the proposed multipole magnetic fields for trapping $\bar{H}$ will actually attract them to the walls. The fraction of $\bar{H}$ formed with negative L_z, needed for possible trapping, is less than expected from statistical arguments.

Without consideration of the needs of forming trappable $\bar{H}$, the rates increase with increasing n. However, the direction of emergence of the Ps (in the first stage) and the wrong sign of the magnetic dipole moment of the $\bar{H}$ (in the second stage) means this method may not produce as many trappable $\bar{H}$ as would be expected from simple estimates. The fact that the two-stage charge exchange in a strong magnetic field gave a distribution of angular momenta unfavorable for trapping leads us to question whether other $\bar{H}$-formation mechanisms have a bias in the resulting angular momentum distribution.

ACKNOWLEDGMENT

This work was supported by the Chemical Sciences, Geosciences, and Biosciences Division of the Office of Basic Energy Sciences, U.S. Department of Energy.

[1] ATHENA Collaboration, M. Amoretti *et al.*, Nature (London) **419**, 456 (2002).
[2] ATRAP Collaboration, G. Gabrielse *et al.*, Phys. Rev. Lett. **89**, 213401 (2002).
[3] G. Gabrielse, S. L. Rolston, L. Haarsma, and W. Kells, Phys. Lett. A **129**, 38 (1988).
[4] M. E. Glinsky and T. M. O'Neil, Phys. Fluids B **3**, 1279 (1991).
[5] F. Robicheaux and J. D. Hanson, Phys. Rev. A **69**, 010701(R) (2004).
[6] F. Robicheaux, Phys. Rev. A **70**, 022510 (2004).
[7] G. Gabrielse *et al.*, Phys. Rev. Lett. **93**, 073401 (2004).
[8] N. Madsen *et al.*, Phys. Rev. Lett. **94**, 033403 (2005).
[9] E. A. Hessels, D. M. Homan, and M. J. Cavagnero, Phys. Rev. A **57**, 1668 (1998).
[10] C. H. Storry *et al.*, Phys. Rev. Lett. **93**, 263401 (2004).
[11] W. H. Press, S. A. Teukolsky, W. T. Vetterling, and B. P. Flannery, *Numerical Recipes*, 2nd ed. (Cambridge University Press, New York, 1992).
[12] The quantity $\mathcal{L}_z$ is conserved for central potentials plus uniform magnetic fields in the z direction; it is even conserved when the magnitude of the magnetic field is time dependent.